Khakim-2014

by Artikel 2 Artikel 2

Lithology-controlled subsidence and seasonal aquifer response in the Bandung basin, Indonesia, observed by synthetic aperture radar interferometry

Mokhamad Yusup Nur Khakim [a,b,*], Takeshi Tsuji [a], Toshifumi Matsuoka [c]

[a] International Institute for Carbon-Neutral Energy Research (WPI-I2CNER), Kyushu University, Japan
[b] Department of Physics, Mathematics and Natural Science Faculty, Sriwijaya University, Indonesia
[c] Department of Urban Management, Kyoto University, Japan

ABSTRACT

Land subsidence in the Bandung basin, West Java, Indonesia, is characterized based on differential interferometric synthetic aperture radar (DInSAR) and interferometric point target analysis (IPTA). We generated interferograms from 21 ascending SAR images over the period 1 January 2007 to 3 March 2011. The estimated subsidence history shows that subsidence continuously increased reaching a cumulative 45 cm during this period, and the linear subsidence rate reached ~12 cm/yr. This significant subsidence occurred in the industrial and densely populated residential regions of the Bandung basin where large amounts of groundwater are consumed. However, in several areas the subsidence patterns do not correlate with the distribution of groundwater production wells and mapped aquifer degradation. We conclude that groundwater production controls subsidence, but lithology is a counteracting factor for subsidence in the Bandung basin. Moreover, seasonal trends of nonlinear surface deformations are highly related with the variation of rainfall. They indicate that there is elastic expansion (rebound) of aquifer system response to seasonal-natural recharge during rainy season.

© 2014 Elsevier B.V. All rights reserved.

1. Introduction

The Bandung basin on the island of Java in West Java Province, Indonesia, has an area of 2340 km^2 and elevations between 660 and 2750 m above sea level. This basin is in the central part of the Bandung zone, a belt of intramontane depressions extending through the center of West Java (Fig. 1). The population of the Bandung metropolitan area was 6.1 million in 2003, and it is predicted to increase to 9.7 million in 2025 (Wangsaatmaja et al., 2006). The growth in population and industrialization, particularly the textile industry, has increased the exploitation of groundwater in the Bandung basin (Wangsaatmaja et al., 2006). Converting agricultural land to housing and industrial sites has worsened environmental impacts (Suhari and Siebenhuer, 1993), and excessive groundwater extraction in the Bandung basin has induced decrease in

groundwater level and as a consequence land subsidence occurred. Decrease in groundwater level in the Bandung basin was reported, for example by Iwaco and Waseco (1990). Abidin et al. (2008) reported that land subsidence in the Bandung basin might be caused by several mechanisms, such as excessive groundwater extraction, building loads, sediment compaction, and tectonic activity.

Studies of subsidence due to groundwater extraction have been carried out using GPS observations in Bandung (Abidin et al., 2008) as well as other sites, such as the Rafsanjan plain, Iran (Mousavi et al., 2001), Po Valley, Italy (Bitelli et al., 2000), and Tianjin, China (Lixin et al., 2011). Although GPS surveys can provide subsidence information with high accuracy, they are costly and time consuming, and they offer sparse spatial resolution in inaccessible areas. In this study, we have applied differential synthetic aperture radar interferometry (DInSAR) as well as interferometric point target analysis (IPTA) to investigate the history of land subsidence of the Bandung basin on a synoptic basis over a 4-year period. The resulting subsidence maps revealed by DInSAR were then combined with other data, such as production well and aquifer damage maps, to characterize the subsidence from a geological point of view. Sri Sumantyo et al. (2012) reported that the subsidence in Indonesia

* Corresponding author at: International Institute for Carbon-Neutral Energy Research (WPI-I2CNER), Kyushu University, Kyushu 819-0395, Japan.
Tel.: +81 92 802 0395.
E-mail addresses: myusup_nkh@i2cner.kyushu-u.ac.jp, myusup_nkh@yahoo.com (M.Y.N. Khakim).
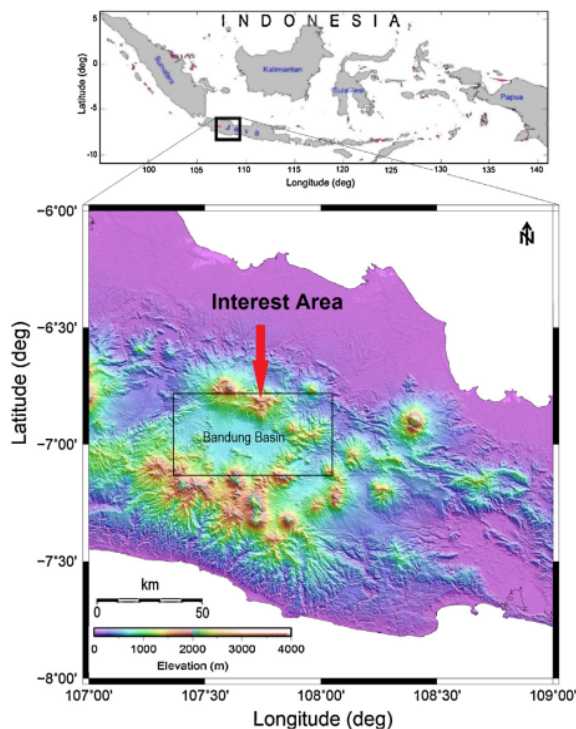
Fig. 1. Location of study area.

is related to the changes in the ground water level due to water pumping, growth in population, industry, and urbanization of the study area. In addition to the water level, furthermore, lithology had been cited as controlling the northern extent of subsidence (e.g., Sneed and Brandt, 2007). Because IPTA further provides information of the time-varying nature of aquifer system compaction, we investigated the factors spatially and temporally controlling subsidence in this area.

2. Data and methods

DInSAR is a means of remote sensing that enables changes in the two-dimensional surface of the Earth to be detected at millimeter to centimeter scales (Massonnet and Feigl, 1998). With applications to natural and artificial sources of deformation such as earthquakes, volcanoes, and land subsidence from groundwater extraction, as well as land uplift from steam injection at oil sand field, InSAR allows us to better understand and analyze the underlying sources of these changes (e.g., Kobayashi et al., 2011; Khakim et al., 2012, 2013; Ishitsuka et al., 2012; Tsuji et al., 2009).

We used raw (level 1.0) SAR data acquired by the Phase Array type L-band (PALSAR) instrument on the Japanese Advanced Land Observation Satellite (ALOS) "Daichi" for the period from 14 January 2007 to 12 March 2011. Data modes are high-bandwidth (FBS-HH, 28 MHz) and low-bandwidth (FBD-HH and HV, 14 MHz) modes, acquired from ascending orbits with an off-nadir angle of 34.3°. Main advantage of the L-band ALOS over C-band ERS is deeper penetration in vegetated areas with less temporal decorrelation enabling to have longer time separation and longer critical baseline, thus it results more usable interferometric pairs (Wei and Sandwell, 2010).

InSAR processing in this study is accomplished with the exception of the lookup table refinement and quadratic phase removal approaches (Khakim et al., 2013). To eliminate the potential of slightly differing azimuth image geometry and maintain coherency, all images were processed using a common Doppler centroid frequency of 63.465 Hz. A global master Single Look Complex (SLC) image for 1 March 2007 was selected that was 9640 pixels wide and 24,705 pixels long, to which all other SLC images were then co-registered. To optimize correlations, the azimuth common band filtering prior to generating interferograms retained only the common segment of the azimuth image spectrum (Ferretti et al., 2007). We applied a two-pass differential InSAR (DInSAR) approach to map land subsidence (Massonnet and Feigl, 1998), using a Shuttle Radar Topography Mission digital elevation model with 3-arcsecond resolution to remove topographic fringes. Adaptive filtering (Li et al., 2006a) was used to reduce the phase noises that cause pseudo phase residues and strongly affect phase unwrapping. The minimum cost flow (MCF) algorithm (Costantini, 1998) was used to minimize areas of low coherence due to layovers and areas of shadowing due to rough terrain.

The mountains surrounding the Bandung basin may impose an altitude dependence on the atmospheric path delay as a result of changes in atmospheric water vapor and pressure above the basin and its surroundings. We therefore generated a phase model of the height-dependent atmospheric phase delay for each unwrapped interferogram and then subtracted it from each interferogram (Li et al., 2006b).

Multiple interferograms were stacked to emphasize temporally coherent signals (including subsidence) and estimate a subsidence rate. Stacking also reduced atmospheric artifacts and phase noise, which are spatially but not temporally coherent. The stacking was done as a weighted sum of individual differential phases using the time interval of the interferogram as the weight (Sandwell and Price, 1998). Longer time intervals yield larger cumulative displacements, making the ratio of phase noise to the differential phase small. Thus, selecting interferograms with long intervals and short baselines yields better results in the stacking calculation.

In order to confirm the resulting subsidence rate obtained by stacking DInSAR data, we applied IPTA (Werner et al., 2003). We also exploited the temporal and spatial characteristics of linear and nonlinear displacements using IPTA. Furthermore, seasonal variation of subsidence trend was extracted using nonlinear least square method with trust-region algorithm (Conn et al., 2000). We first subtracted the known linear displacement from total displacement of each time series to estimate seasonal amplitudes. More details to estimate both linear and nonlinear components of displacement based on IPTA is described in Wegmuller et al. (2004, 2008). Nonlinear trends $y(t)$ are then fit to a Fourier series model, instead of a simple-sinusoidal model (Bell et al., 2008), to each time series as follows,

$$y(t) = a_0 + \sum_{n=1}^{4} a_n \cos(n\omega t) + b_n \sin(n\omega t) \qquad (1)$$

where a_0 is a constant shift in the model due to interferometric noise, a_n and b_n are the maximum seasonal amplitude for either subsidence or uplift oscillations, t and ω are time and angular frequency of subsidence or uplift oscillation, respectively. For the seasonal analysis we assumed around 1-year periodicity for initial parameters for inversion, because the ground deformation (uplift and subsidence) is based on the annual cycles of discharge and recharge processes. Some statistical parameters used to evaluate the fit goodness are sum of squares due to error (SSE), R-square, and root mean squared error (RMSE).
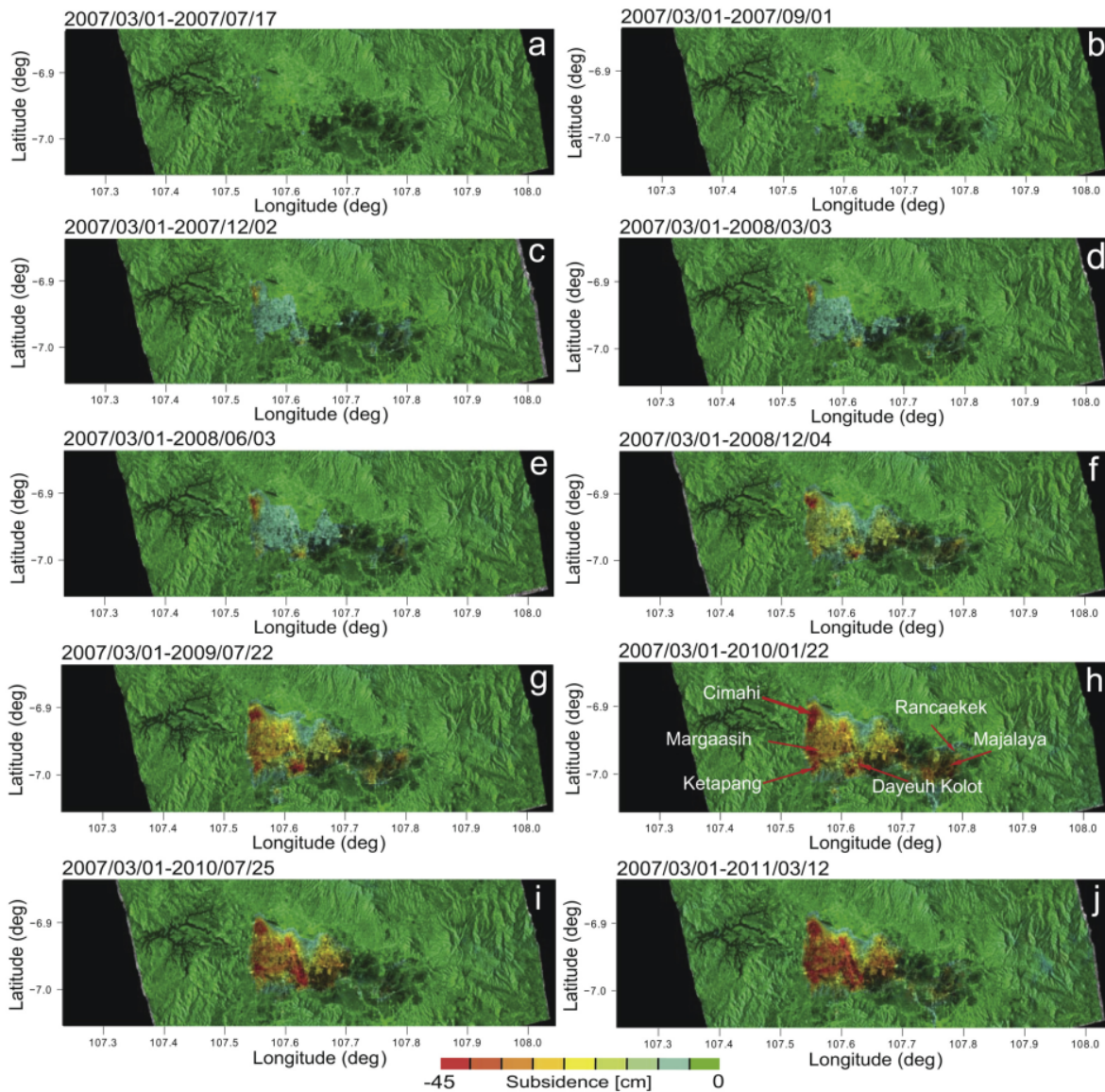
Fig. 2. Sequential subsidence patterns in Bandung basin from 138 days to 1472 days after 1 March 2007.

3. Results and discussion

We mapped of displacement history estimated by using two-repeat pass DInSAR for the period 1 March 2007 to 12 March 2011 with the same baseline of 1 March 2007 (Fig. 2). Based on our analysis, the coherence of generated interferograms is lower in farmland, lake, river, vegetative areas than in urban area. The coherence is more than 0.6 in urban area and less than 0.3 in surrounding area consisting vegetated area. Fortunately, our target area is located in urban area where subsidence occurred. Thus subsidence could be accurately estimated and reasonably good quality for this study.

Subsidence features are generally oriented in the northwest–southeast direction of the Bandung basin itself. Subsidence began historically in several urban areas where industries were established; in our mapping these grew and merged over the study period to create a larger subsidence pattern over the Bandung basin. Subsidence was concentrated in urban areas such as Cimahi, Rancaekek, Dayeuh Kolot, Ketapang, Margaasih, Majalaya (Fig. 2h). Subsidence in the city of Cimahi reached ~45 cm during the study period obtained from the DInSAR technique, for a subsidence rate of ~12 cm/yr. These results agree well with subsidence obtained from IPTA technique (discussed in Section 3.2).

3.1. Spatial variation

Because groundwater extraction has been suspected of contributing to subsidence in the study area, we compared our
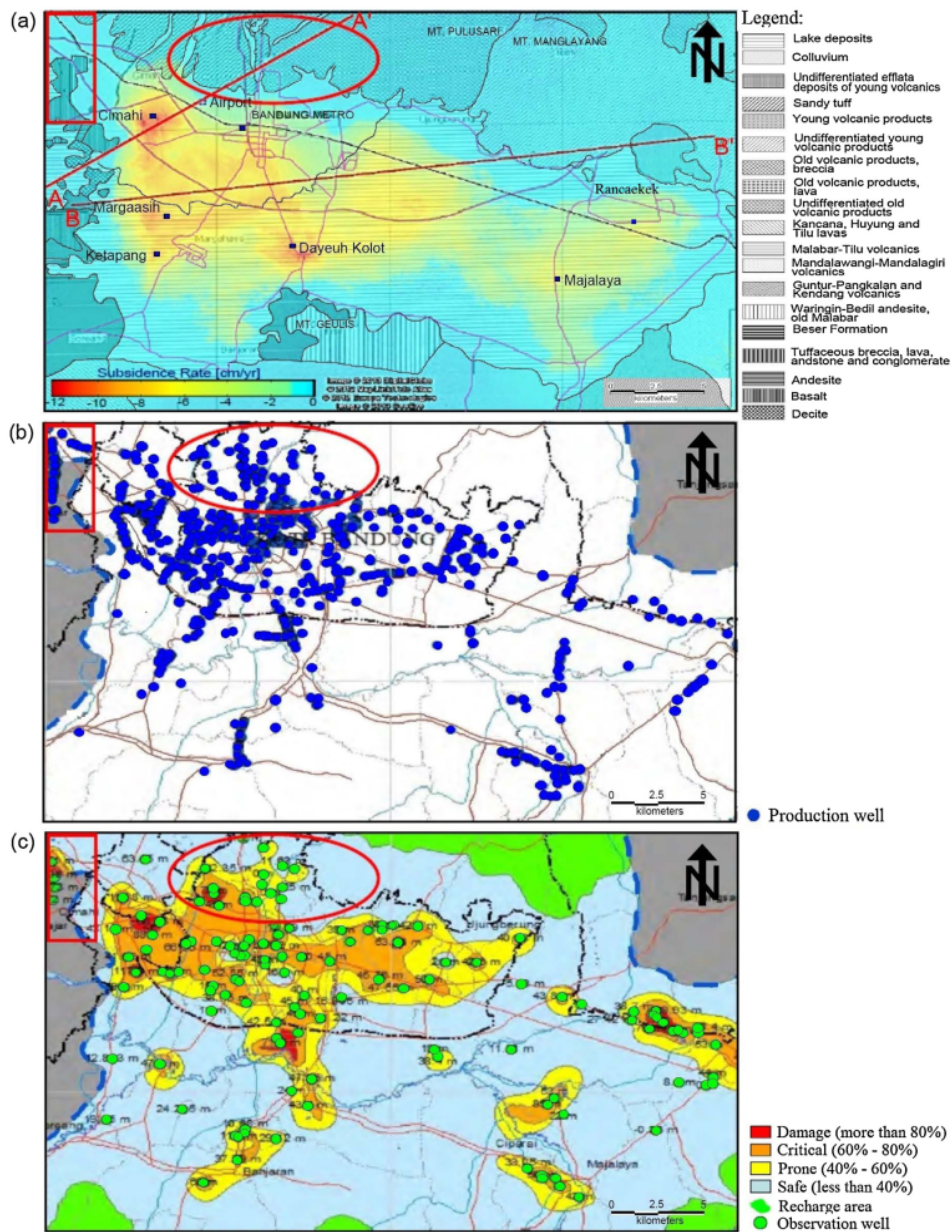
Fig. 3. (a) Subsidence rate overlaid on geologic map of Delinom and Suriadarma (2010). (b) Distribution of groundwater production wells in the Bandung basin. Most wells are in Cimahi and Bandung cities (BPLH and LAPIITB, 2011), (c) aquifer zoning in the Bandung basin based on the percentage of groundwater decline as of 2010 (BPLH and LAPIITB, 2011). (For interpretation of the references to color in this sentence, the reader is referred to the web version of the article.)

subsidence maps (Fig. 3a) to the groundwater production wells and aquifer zonation (Fig. 3b and c) (BPLPH and LAPIITB, 2011). As expected, subsidence was generally associated with areas of greater density of production wells and greater declines in groundwater level. The aquifer was classified by the percentage of its area with groundwater declines into zones labeled "damage", "critical", "prone", and "safe" defined as more than 80%, 60–80%, 40–60%, and less than 40%, respectively (Fig. 3c). For most areas in the Bandung basin, the pattern of estimated subsidence rate is correlated with both the distribution of production wells (Fig. 3b) and aquifer zonation (Fig. 3c). Interestingly, subsidence did not occur in the areas outlined in red in Fig. 3a, even though those areas included damaged aquifers and dense production wells (Fig. 3b and c).

The northeastern part of Cimahi is located on an area of alluvium (as part of unconsolidated Cibeureum Formation) surrounded by consolidated rocks, volcanic products, breccia (Cikapundung Formation) in the northeastern part whereas tuffaceous breccia, lava, sandstone and conglomerate (basement) in the southwestern
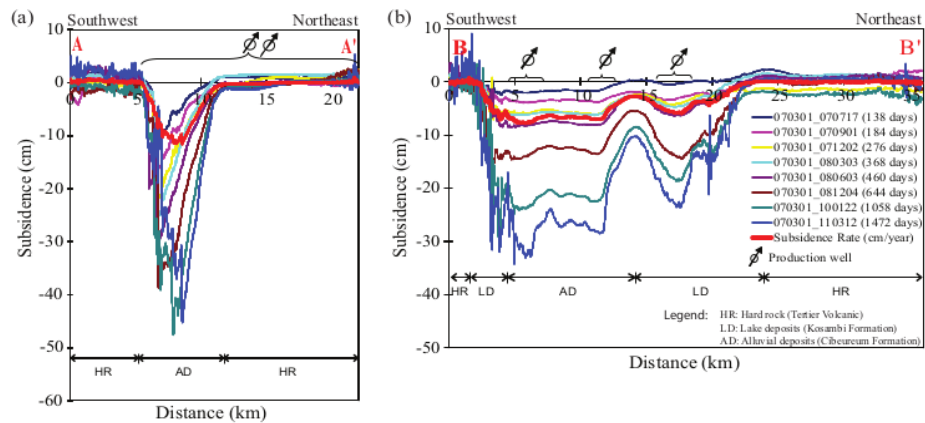
Fig. 4. Profiles of subsidence across Cimahi city (Fig. 3a) obtained from stacking 32 differential SAR interferograms and an individual SAR interferogram with time intervals from 138 to 1472 days after 1 March 2007: (a) line A–A′ and (b) line B–B′. Also shown are subsidence rates along both profiles.

(Fig. 3a). The hydrological condition of Cibeureum Formation is as the highest productivity aquifer in the Bandung basin (Iwaco and Waseco, 1991). Despite a large amount of groundwater extraction in northeastern Cimahi, land subsidence was absent in the area of consolidated rocks. But significant subsidence was observed in areas of alluvium and lake deposits. The lake deposit is a part of stratigraphical unit of Kosambi Formation (Koesoemadinata and Hartono, 1981). It appears that subsidence in this part of the Bandung basin is controlled by lithology. The same was true of several other areas.

We constructed eight time-lapse profiles of subsidence across Cimahi along lines A–A′ and B–B′ (Fig. 3a). These profiles (Fig. 4) indicate that subsidence patterns at all time intervals, from 138 to 1472 days, are highly consistent with each other. This pattern shows that subsidence depends on geological conditions in the aquifer and its surroundings. If the subsurface in the profile is laterally homogeneous, the subsidence should be symmetrical across the profiles. At the southwestern end of profile A–A′ (Fig. 4a), however, the slopes of the subsidence are relatively constant and steep, indicating the presence of a boundary between consolidated rock on the southwest and compressible alluvial sediment on the northeast. The boundary may also act as a barrier to groundwater flow that would impede the horizontal propagation of fluid pressure in water levels.

In the northeastern part of Cimahi and Bandung cities, subsidence was expected as a result of groundwater overpumping where the aquifer map shows a "damage" zone (Fig. 3c). However, there is no subsidence in that region despite the presence of production wells in the northeastern part of profile A–A′ (Fig. 4a). Based on these observations, features in the subsidence map do not correspond with features in the aquifer zoning map in several areas. However, subsidence did not occur in hard rock areas but increased with time in alluvial sediment deposits.

Profile B–B′ (Fig. 4a) crossed the central part of the subsiding area over substrates of hard rock, alluvium, and lake deposits. The corresponding subsidence profiles (Fig. 4b) are also sensitive to the presence of production wells and lithology. Subsidence occurred in areas with no production wells (Fig. 3b) indicates that groundwater extraction has a widespread effect in an area where aquifers are interconnected. However, the peaks in subsidence were always in areas hosting production wells.

Relations between subsidence rates and geologic features are also clearly shown in Fig. 5. Profiles of subsidence rates transect along line C–C′ and D–D′ (index map of Fig. 5) indicating large

subsidence occurred in areas dominated by Cibeureum Formation. This formation is distributed southward in form of Alluvium fan (Koesoemadinata and Hartono, 1981). Undulations in the subsidence profile in Fig. 5a and b are associated with the presence of Citarum and Cikapundung rivers as natural recharges of surface water.

3.2. Seasonal variation

Total deformation of ground surface, which a nonlinear component and noise are superimposed on linear component (blue circles in Fig. 6b–g), indicates that the fluctuations of deformations varied with time. Even though cyclic uplift occurred, subsidence trends continuously and linearly increased in magnitude. Linear-subsidence rates estimated by using IPTA agree well with those of DInSAR. The linear displacement rates obtained from IPTA in several areas, such as Cimahi, Dayeuh Kolot, Rancaekek, Margaasih, Ketapang, and Majalaya with the rates of 11.9 cm/yr, 8.6 cm/yr, 6.1 cm/yr, 5.6 cm/yr, 7.4 cm/yr, and 7.4 cm/yr, respectively (Fig. 6b–g) by fitting a linear regression ($R^2 > 0.95$).

To investigate characteristics of aquifer system response to seasonal variations, we derived components of nonlinear deformation by using IPTA. This analysis provides insight into the elastic deformation of the aquifer system. Using trust-region algorithm with the 95% confidence interval, we evaluated the fit goodness of data to the model when estimating seasonal displacement trends (Fig. 7). From this evaluation, the model has small random error components. It can be indicated from SSE values closed to zero (i.e., 0.0029, 0.0046, 0.0014, 0.0017, 0.0013, and 0.0022). A maximum R-square value is up to 0.7 indicating that the fit explains 70% of total variation in the data about the average. In addition, the standard deviation of the random component in the data ranges from 0.01 to 0.02. It indicates that the fits are useful for our analysis.

Estimated trends of nonlinear subsidence are highly related with the variation of rainfall over the Bandung basin as shown in Fig. 7. This relationship is important information for inferring aquifer system behavior during groundwater extraction. Aquifer-system deformation in the elastic range of stress typically is small and reversible (Galloway and Sneed, 2013). Seasonal, reversible land surface displacements (subsidence and uplift) of a few cm are typical for many alluvial aquifer systems with significant fractions of fine-grained deposits. It can be understood that when fluid is injected pore pressure rises and possibly exceeds the original value. In this case the effective stress decreases under the original value.
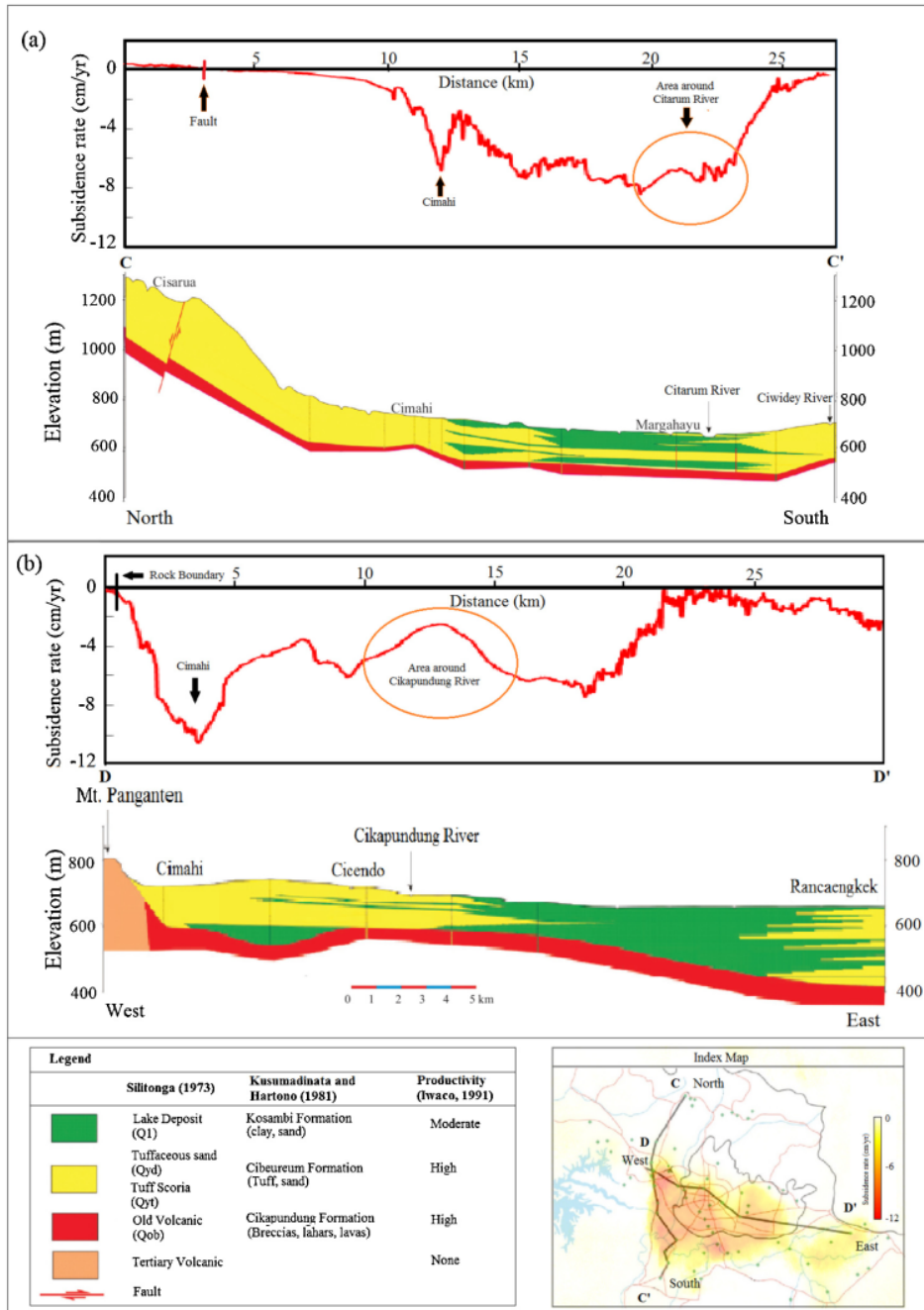
Fig. 5. Relations between profiles of subsidence rate and lithological sections: (a) line C–C' (north–south direction) and (b) line D–D' (west–east direction).
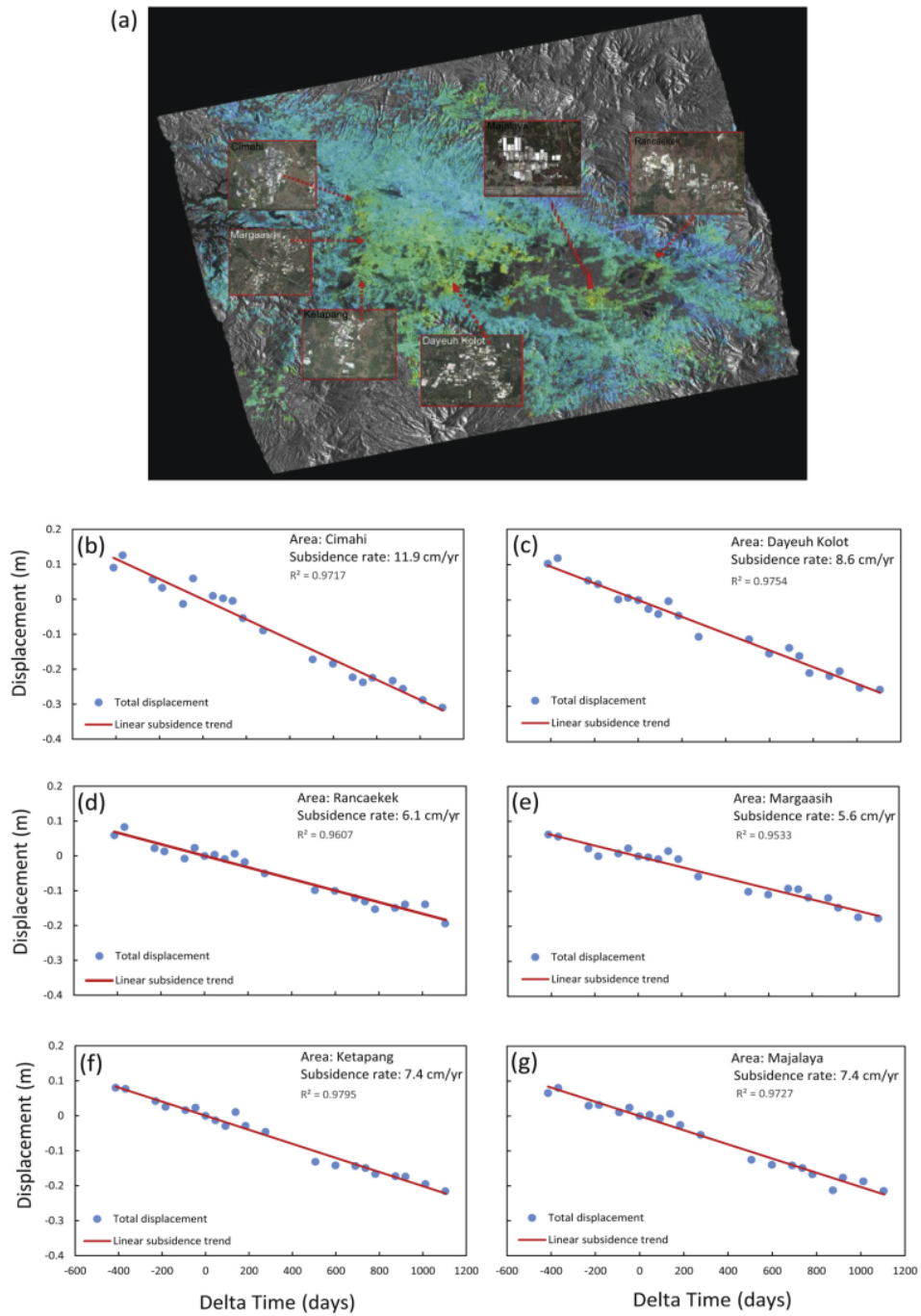
Fig. 6. The results of IPTA: (a) linear displacement map, (b)–(g) linear displacement trends for Cimahi, Dayeuh Kolot, Rancaekek, Margaasih, Ketapang, and Majalaya, respectively. Blue dots indicate total displacement data including linear, nonlinear, and noise components. Red lines are the trend of linear subsidence estimated using regression linear from data. (For interpretation of the references to color in this figure legend, the reader is referred to the web version of the article.)
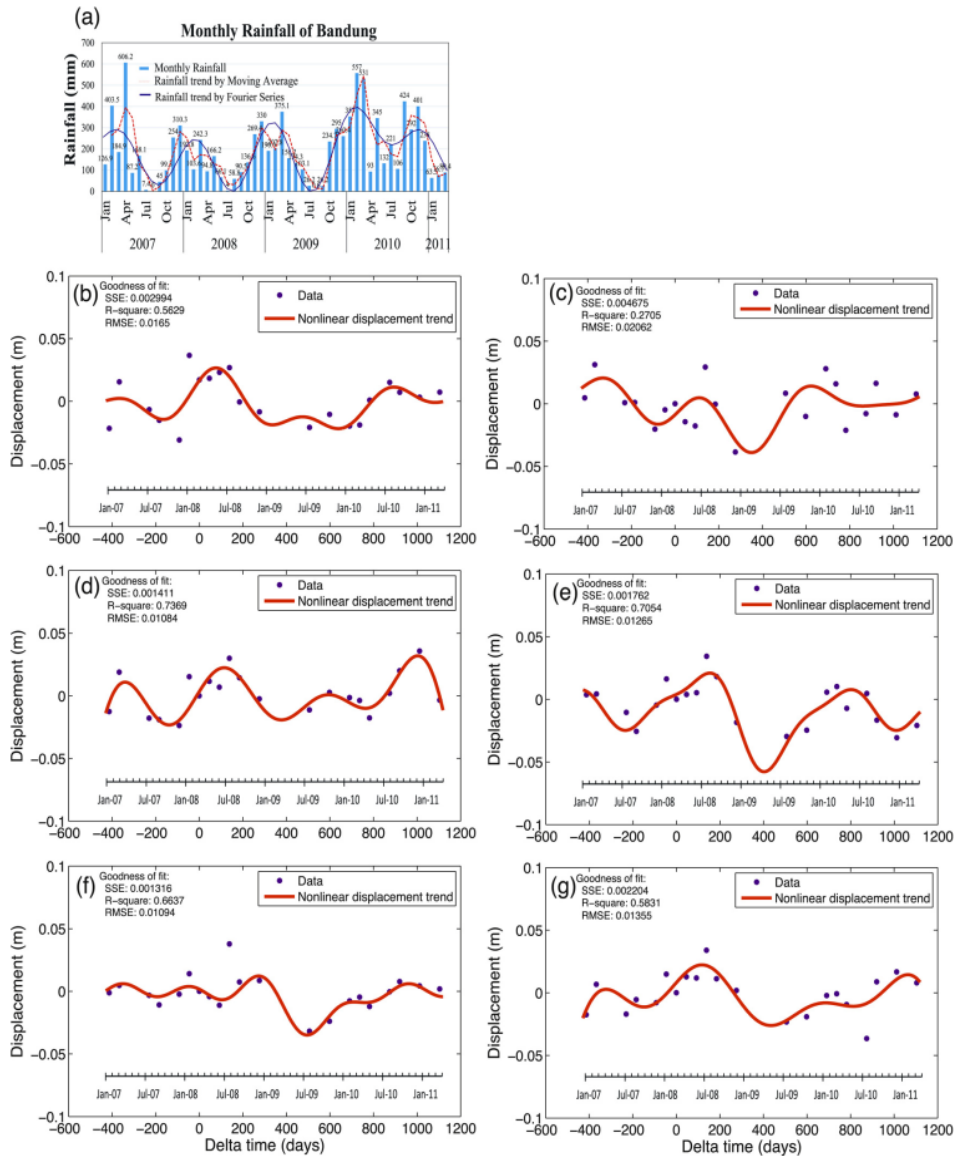
Fig. 7. (a) The variation of monthly rainfall in Bandung basin from January 2007 to March 2011 (Mangindaan, 2012). (b)–(g) Nonlinear displacement trends for Cimahi, Dayeuh Kolot, Rancaekek, Margaasih, Ketapang, and Majalaya, respectively.

Moreover, a dilatation phenomenon could be induced, thus contributing to the magnitude of the injected formation expansion. A more detailed description of the land uplift (rebound) mechanism due to fluid injection was given by Teatini et al. (2011).

In the Bandung basin, seasonal uplifts, of up to 2–4 cm, (Fig. 7b–g) reflected elastic expansion of the aquifer system response to groundwater level recovery during rainy season (October–March). During this season any residual compaction in the aquifer system generally is compensated by elastic expansion in the aquifers and aquitards as natural recharging response, thus resulting in a subsidence reduction. However, this natural recharge rate may be less than groundwater discharge, and then a net displacement becomes subsidence. Therefore, this natural recharge is not significant to recover aquifer system from compaction. Meanwhile, in the dry season (April–September) when groundwater level decline, aquifer systems undergo a compaction (no rebound) as a consequence of groundwater discharge.

Based on seasonal deformation trends, the aquifer has characteristics to retain an elastic expansion. It has potential to recover some storage capability under enhanced future management (Amelung et al., 1999; Osmanoglu et al., 2010). During rainy season, annual uplift occurred indicating that aquifer rebounded due to recharging from surface water. Therefore, seasonal deformation trends derived from SAR data provide information of elastic expansion of the naturally or artificially injected formation.

4. Conclusion

We successfully used the DInSAR and IPTA techniques to derive rates, spatial details, and temporal variations of land subsidence associated with groundwater extraction in the Bandung basin, West Java, Indonesia. Areas of subsidence that initially arose in industrialized urban areas extended in space and increased in magnitude over the period of our survey. The rate of subsidence was as much as 12 cm/yr.

The magnitude and patterns of subsidence are not perfectly correlated with the distribution of groundwater production wells and groundwater levels. Abrupt changes in the subsidence degree were observed at boundaries between consolidated rock and unconsolidated sediment in the basin. Subsidence did not occur in response to groundwater withdrawal in areas of consolidated rocks. We conclude that subsidence in Bandung basin is controlled not only by groundwater withdrawal, but also by lithological factors.

Although subsidence was reduced by the elastic expansion of the aquifer system response to natural recharge during rainy season, residual compaction continued affecting further subsidence. Natural recharge cannot recover aquifer system from compaction.

References

Abidin, H.Z., Andreas, H., Gamal, M., Wirakusumah, A.D., Darmawan, D., Deguchi, T., Maruyama, Y., 2008. Land subsidence characteristics of the Bandung basin, Indonesia, as estimated from GPS and InSAR. J. Appl. Geodesy 2 (3), 167–177, http://dx.doi.org/10.1515/JAG.2008.019.

Amelung, F., Galloway, D.L., Bell, J.W., Zebker, H.A., Laczniak, R.J., 1999. Sensing the ups and downs of Las Vegas: InSAR reveals structural control of land subsidence and aquifer-system deformation. Geology 27, 483–486.

Bell, J.W., Amelung, F., Ferretti, A., Bianchi, M., Novali, F., 2008. Permanent scatterer InSAR reveal seasonal and long-term aquifer-system response to groundwater pumping and artificial recharge. Water Resour. Res. 44 (W02407), 1–18, http://dx.doi.org/10.1029/2007WR006152.

Bitelli, G., Bonsignore, F., Unguendoli, M., 2000. Levelling and GPS networks for ground subsidence monitoring in the southern Po Valley. J. Geodyn. 30 (3), 355–369, http://dx.doi.org/10.1016/S0264-3707(99)00071-X.

BPLH (Badan Pengelolaan Lingkunga Hidup Daerah) and LAPIITB (Lembaga Afiliasi Penelitian dan Industri Institute Teknologi Bandung), 2011. Naskah akademik raperda kota Bandung tentang pengelolaan air tanah (Academic Manuscript of local Regulation Draft for Bandung City on Groundwater Management). Laporan Akhir, BPLH Kota Bandung, Bandung.

Conn, A.R., Gould, N.I.M., Toint, P.L., 2000. Trust-Region Methods, SIAM Society for Industrial & Applied Mathematics. Englewood Cliffs, New Jersey.

Costantini, M., 1998. A novel phase unwrapping method based on network programming. IEEE Trans. Geosci. Remote Sens. 36 (3), 813–821, http://dx.doi.org/10.1109/36.673674.

Delinom, R.M., Suriadarma, A., 2010. Groundwater flow system of Bandung basin based on hydraulic head, subsurface temperature, and stable isotopes. Riset Geologi dan Pertambangan 20 (1), 55–68.

Ferretti, A., Monti-Guarnieri, A., Prati, C., Rocca, F., 2007. InSAR Principles: Guidelines for SAR Interferometry Processing and Interpretation. ESA.

Galloway, D.L., Sneed, M., 2013. Analysis and simulation of regional subsidence accompanying groundwater abstraction and compaction of susceptible aquifer systems in the USA. Boletin De La Sociedad Geologica Mexicana 65 (1), 123–136.

Ishitsuka, K., Tsuji, T., Matsuoka, T., 2012. Detection and mapping of soil liquefaction associated with the 2011 Tohoku earthquake using SAR Interferometry. Earth Planets Space 64, 1267–1276.

Iwaco, Waseco, 1990. West Java Provincial Water Source Master Plan For Water Supply, Kabupaten Bandung; Vol. A: Groundwater Resources, and Vol. B: Master Plan for Water Supply, Jakarta.

Iwaco, Waseco, 1991. Bandung Hydrological Study, West Java Provincial Water Resources Master Plan, Jakarta.

Khakim, M.Y.N., Tsuji, T., Matsuoka, T., 2012. Geomechanical modeling for InSAR-derived surface deformation at steam-injection oil sand fields. J. Pet. Sci. Engineering 96–97, 152–161, http://dx.doi.org/10.1016/j.petrol.2012.08.003.

Khakim, M.Y.N., Tsuji, T., Matsuoka, T., 2013. Detection of localized surface uplift by differential SAR interferometry at the hangingstone oil sand field, Alberta, Canada. IEEE J. Sel. Top. Appl. Earth Observ. Remote Sens. 6 (6), 2344–2354, http://dx.doi.org/10.1109/JSTARS.2013.2254471.

Kobayashi, T., Tobita, M., Nishimura, T., Suzuki, A., Noguchi, Y., Yamanaka, M., 2011. Crustal deformation map for the 2011 off the Pacific coast of Tohoku Earthquake, detected by InSAR analysis combined with GEONET data. Earth Planets Space 63, 621–625.

Koesoemadinata, R.P., Hartono, D., 1981. Stratigrafi dan sedimentasi daerah Bandung. In: Prosiding Ikatan Ahli Geologi Indonesia, (Proceedings of the Annual Meeting of Indonesian Association of Geologist).

Li, Z.W., Ding, X.L., Huang, C., Zheng, D.W., Zou, W.B., Shea, Y.K., 2006a. Filtering method for SAR interferograms with strong noise. Int. J. Remote Sens. 27, 2991–3000, http://dx.doi.org/10.1080/01431160500522692.

Li, Z.W., Ding, X.L., Huang, C., Wadge, G., Zheng, D.W., 2006b. Modeling of atmospheric effects on InSAR measurements by incorporating terrain elevation information. J. Atmos. Solar-Terrest. Phys. 68 (11), 1189–1194, http://dx.doi.org/10.1016/j.jastp.2006.03.002.

Lixin, Y., Fang, Z., He, Z., Shijie, C., Wei, W., Qiang, Y., 2011. Land subsidence in Tianjin, China. Environ. Earth Sci. 62 (6), 1151–1161, http://dx.doi.org/10.1007/s12665-010-0604-5.

Mangindaan, E.E., 2012. Transportation Statistics 2011, Book II. Ministry of Transportation, Indonesia.

Massonnet, D., Feigl, K., 1998. Radar interferometry and its application to changes in the Earth's surface. Rev. Geophys. 36 (4), 441–500, http://dx.doi.org/10.1029/97RG03139.

Mousavi, S.M., Shamsai, A., Naggar, M.H., Khamehchian, M., 2001. A GPS-based monitoring program of land subsidence due to groundwater withdrawal in Iran. Can. J. Civil Eng. 28 (3), 452–464, http://dx.doi.org/10.1139/l01-013.

Osmanoglu, B., Dixon, T.H., Wdowinski, S., Cabral-Cano, E., Jiang, Y., 2010. Mexico city subsidence observed with persistent scatterer InSAR. Int. J. Appl. Earth Observ. Geoinf. 13 (1), 1–12.

Sandwell, D.T., Price, E.J., 1998. Phase gradient approach to stacking interferograms. J. Geophys. Res. 103 (B12), 30183–30204, http://dx.doi.org/10.1029/1998JB900008.

Sneed, M., Brandt, J., 2007. Detection and Measurement of Land Subsidence using Global Positioning System Surveying and Interferometric Synthetic Aperture Radar, Coachella Valley, California, 1996–2005: U. S. Geological Survey Scientific Investigations Report 2007-5251. USGS, California.

Sri Sumantyo, J.T., Shimada, M., Mathieu, P.P., Abidin, H.Z., 2012. Long-term consecutive DInSAR for volume change estimation of land deformation. IEEE Trans. Geosci. Remote Sens. 50, 259–270.

Suhari, S., Siebenhuer, M., 1993. Environmental geology for land use and regional planning in the Bandung basin, West Java, Indonesia. J. Southeast Asian Earth Sci. 8 (1–4), 557–566, http://dx.doi.org/10.1016/0743-9547(93)90053-R.

Teatini, P., Gambolati, G., Ferronato, M., Settari, A, Walters, D., 2011. Land uplift due to subsurface fluid injection. J. Geodyn. 51, 1–16.

Tsuji, T., Yamamoto, K., Matsuoka, T., Yamada, Y., Onishi, K., Bahar, A., Meilano, I., Abidin, H.Z., 2009. Earthquake Fault of the 26 May 2006 Yogyakarta Earthquake Observed by SAR Interferometry. Earth Planets Space (E-Letter) 61, e29–e32.

Wangsaatmaja, S., Sutadian, A.D., Prasetiati, M.A.N., 2006. Sustainable Groundwater Management In Asian Cities: A Summary Report of Research on Sustainable Water Management in Asia. Institute for Global Environmental Strategies (IGES), Japan.

Wegmuller, U., Werner, C., Strozzi, T., Wiesmann, A., 2004. Multi-temporal interferometric point target analysis. Analysis of multi-temporal remote sensing images. In: Smits, P.C., Bruzzone, L. (Eds.), Series in Remote Sensing, vol. 3. World Scientific, pp. 136–144, ISBN 981-238-915-61.

Wegmuller, U., Walter, D., Spreckels, V., Werner, C., 2008. Evaluation of TerraSAR-X DINSAR and IPTA for ground motion monitoring. In: Proceedings of the Third TerraSAR-X Science Team Meeting, 25–26 November 2008, DLR, Oberpfaffenhofen, Germany.

Wei, M., Sandwell, D.T., 2010. Decorrelation of L-band and C-band interferometry over vegetated areas in California. IEEE Trans. Geosci. Remote Sens. 48 (7), 2942–2952.

Werner, C., Wegmuller, U., Strozzi, T., Wiesmann, A., 2003. Interferometric point target analysis for deformation mapping. In: Geoscience and Remote Sensing Symposium, IGARSS'03. Proceedings. 2003 IEEE International, vol. 7, pp. 4362–4364.

Khakim-2014